

A tellurium-substituted Lindqvist-type polyoxoniobate showing high H₂ evolution catalyzed by tellurium nanowires *via* photodecomposition†

Cite this: *Chem. Commun.*, 2014, 50, 836

Received 12th September 2013,
Accepted 12th November 2013

DOI: 10.1039/c3cc47001f

Jung-Ho Son,^{*a} Jiarui Wang,^a Frank E. Osterloh,^a Ping Yu^b and William H. Casey^{*ac}

www.rsc.org/chemcomm

A new tellurium-substituted Lindqvist-type polyoxoniobate [H₂TeNb₅O₁₉]^{5−} was synthesized as a tetramethylammonium salt. When irradiated with a Xe lamp, a water–methanol solution of this cluster showed exceptionally high H₂-evolution activity suggesting cocatalysis by the hexaniobate cluster and metallic tellurium, both of which are formed as photodecomposition products.

The most common aqueous complexes of Nb^V are the hexaniobate Lindqvist ion (Nb₆) and the decaniobate ion and these two clusters dominate in different pH regions.¹ Heterometal-substituted Lindqvist-type polyoxoniobate ions are virtually unknown and the single example is the tungsten-rich [HNb₂W₄O₁₉]^{3−} ion.² Herein we report a tellurium-monosubstituted Lindqvist-type polyoxoniobate ion as a tetramethylammonium (TMA) salt, TMA₅[H₂TeNb₅O₁₉]·20H₂O (**1**). This molecule is important for two reasons, firstly because ¹²⁵Te is an NMR-active nucleus with spin 1/2 and a long relaxation time, allowing study of aqueous chemistry in ways that were difficult with the unsubstituted hexaniobate ion, wherein only ¹⁷O NMR could be used as an NMR probe to solution chemistry,³ and secondly because the molecule photodecomposes to a catalytic system for H₂ production, as shown in this study. Although the niobate Lindqvist ion is well known, its utility in the field of hydrogen energy is not well investigated. Here we demonstrated that Te-substitution of the Lindqvist ion can generate a highly active photocatalytic system in comparison to the pristine Lindqvist hexaniobate ion.

Tellurium substitution has been previously achieved in other polyoxometalate systems including Anderson-type [TeMo₆O₂₄]^{6−} clusters, *trans*-disubstituted Lindqvist-type [Te₂Mo₄O₁₉]^{6−} clusters and decavanadate-type [HTeV₉O₂₈]^{4−} clusters.^{4,5} A mixed oxide of molybdenum, vanadium, tellurium and niobium has been shown to be a good catalyst for conversion of hydrocarbons; thus the tellurium-substituted niobate ion has potential to act as a catalytically active oxide precursor.^{4a,5a} Solid niobates have also been studied as water-splitting photocatalysts, along with more effective and well-known titanates and tantalates,⁶ as niobium oxides have a bandgap energy of about 3.4 eV and that compares well to ZnO or TiO₂.⁷ Photocatalytic H₂ evolution activities of oligomeric polyoxoniobates have been reported recently.⁸

The synthesis of **1** was carried out by a hydrothermal reaction of a mixture of Te(OH)₆ (telluric acid), hydrous niobium oxide and TMAOH. Electrospray-ionization mass spectrometry (ESI-MS) of the solution after reaction suggested the formation of a new Te-substituted cluster, as proven by the complex fingerprint of each peak due to the naturally occurring Te isotopes and higher *m/z* values compared to the TMA salt of hexaniobate, TMA₅[H₃Nb₆O₁₉]·20H₂O (**2**) [Fig. S1, S4 and S5, ESI†]. The peak positions match well with calculated peaks of the TMA salt of Te-monosubstituted hexaniobate [Fig. S1, ESI†].

The structure of [H₂TeNb₅O₁₉]^{5−} (TeNb₅) in **1** was determined by X-ray single crystallography [Fig. 1].‡ The tellurium substitution is obvious from the high electron density in one (Te1/Nb1 site) of the three crystallographically independent metal sites. Tellurium is disordered between the two opposite metal sites in the Lindqvist ion due to its centrosymmetry. Refinement with the partial occupancy model at the Te1/Nb1 site showed that the sum of tellurium occupancy in these two sites is 0.95, which is in good agreement with the suggested TeNb₅ stoichiometry. Two protons are bound on the two opposite μ₂-O, linking Nb2 and Nb3 on the equatorial plane. Five TMA counteranions are found in the structure refinement, and the formula is expressed as TMA₅[H₂TeNb₅O₁₉]·20H₂O. The cell constants are very similar to those of the previously reported **2**,⁹ which is in agreement with the isostructural and isovalent Lindqvist-type cluster

^a Department of Chemistry, University of California, Davis, One Shield Ave., Davis, CA 95616, USA. E-mail: junghoson@gmail.com, whcasey@ucdavis.edu;
Fax: +1 530 752 8995; Tel: +1 530 752 3211

^b Keck NMR Facility, University of California, Davis, One Shields Ave., Davis, CA 95616, USA

^c Department of Geology, University of California, Davis, One Shield Ave., Davis, CA 95616, USA

† Electronic supplementary information (ESI) available: Synthesis details, instrumental analysis conditions, ESI-MS spectrum of **1**, crystal packing diagram, FT-IR spectra of **1**, **2** and **3**, pH dependent ESI-MS and UV-Vis spectra of **1** and **2**, SEM and XRD of tellurium precipitate. CCDC 959006. For ESI and crystallographic data in CIF or other electronic format see DOI: 10.1039/c3cc47001f



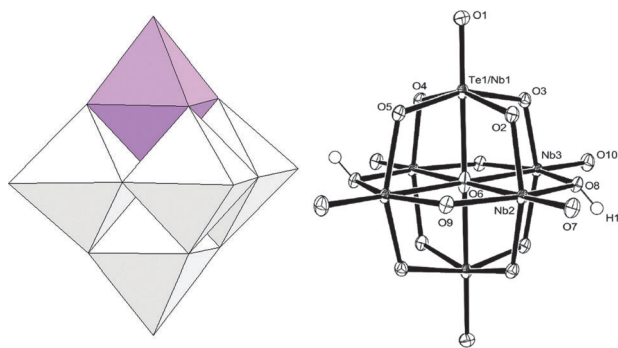


Fig. 1 Polyhedral model (left, Te^{VI}: purple, Nb^V: white) and thermal-ellipsoid model of [H₂TeNb₅O₁₉]⁵⁻ (right). Unlabelled atoms are related to the labelled atoms by inversion symmetry.

crystallized with the same number of TMA counteranions and crystallization water. As a result of the substitution, the terminal Te/Nb–O_t bond (1.8082(12) Å) is longer than the unsubstituted terminal Nb–O_t bond in the periphery (1.7505(11) and 1.7727(11) Å). And the Te/Nb–μ₆-O bond (2.28325(15) Å) is shorter than Nb–μ₆-O bonds (2.41480(16) and 2.44065(15) Å). Because of the mixed metal occupancy, thermal ellipsoids of Te1/Nb1 and μ₆-O are elongated in the axial direction [Fig. 1].

Solid-state ¹²⁵Te NMR experiment was performed to characterize the Te^{VI} in the cluster. The single substitution in TeNb₅ suggests one peak. As predicted, solid-state ¹²⁵Te NMR spectrum shows one isotropic peak at 754 ppm accompanied with spinning sidebands [Fig. 2]. We note that the spinning sidebands are not symmetric about the central isotropic peak because Te is in an asymmetric structural environment. The Te is located at one metal site of the Lindqvist cluster, which is intrinsically asymmetric, and faces the center of the cluster on one side, while the other side is coordinated with the terminal oxygen atom and is closer to TMA ions and crystallization waters [Fig. 1, Fig. S2, ESI†].

The pH-dependent stabilities of **1** and **2** were examined by performing ESI-MS and UV-Vis titration experiments. ESI-MS spectra of 31 mM solution (pH = 8.1) of each compound were

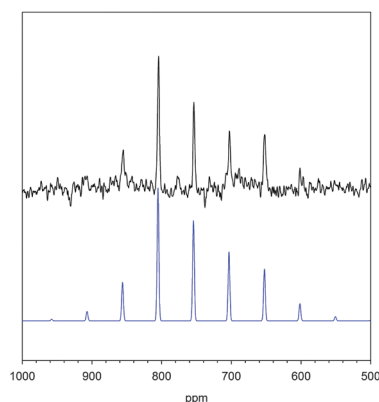


Fig. 2 The ¹²⁵Te MAS NMR spectrum (top) can be fitted with a CSA pattern at a spinning speed of 8 kHz (bottom). The axiality of the CSA is –160 ppm, the asymmetry parameter is 0.56, the peak width is 300 Hz, and the isotropic chemical shift is 754.3 ppm. These parameters describe the local coordination environment of the Te^{VI} site.

recorded after the addition of acid or base to modify the solution pH. The peaks of **1** only slightly decreased up to pH ~ 13 when titrated with base, indicating that the TeNb₅ cluster is stable under strongly basic conditions [Fig. S4, ESI†]. When titrated with acid, the solution became cloudy, and increasingly so, upon addition of each aliquot below pH 7, which was probably due to formation of hydrous niobium-oxide colloids. However, most of the clusters in solution had converted to colloidal particles at pH ~ 5 and below. ESI-MS titration of **2** showed similar behaviour [Fig. S5, ESI†]; Nb₆ was stable between 7 < pH < 12 but less stable under extreme pH conditions, as suggested by normalized abundance of representative peaks in ESI-MS depending on pH [Fig. S6, ESI†]. In the UV-Vis titration experiment using a more dilute solution (0.03 mM), the electronic spectra of **1** which show LMCT bands at 240 nm and small shoulder at 265 nm did not change significantly up to pH 12.5, which agrees with the stability of TeNb₅ under the basic conditions [Fig. S7, ESI†]. During the titration with acid, the overall absorption increased up to pH ~ 4, which is indicative of decomposition. A solution of **2** showed a similar trend in the UV-Vis titration [Fig. S8, ESI†].

We examined photochemical H₂ evolution from each 0.2 g of **1** and **2** in a water-methanol solution (25 mL, 80 : 20 v/v) under UV and visible light from a 300 W Xe lamp. Hydrogen evolution activity of TMA salt of peroxohexaniobate, TMA₅[H₃Nb₆O₁₃(O^{II}₂)₆]·9.5H₂O (**3**),⁹ was also measured. Methanol was used as a sacrificial electron donor and H₂ was monitored by gas chromatography. Visible light (>400 nm) did not produce H₂; however, under full Xe spectrum illumination a solution of **1** evolved H₂ at a rate of 776 μmol h⁻¹ g⁻¹, which is 70 times higher than that of **2** (11 μmol h⁻¹ g⁻¹) [Fig. 3]. Upon irradiation, the solution of **2** remained colorless while the solution of **1** became gradually darker and about 10 mg of a black precipitate formed after 8 hours, which was identified as metallic tellurium in mostly nanowire morphology mixed with some microcrystals, on the basis of SEM and XRD data (Fig. S9 and S10, ESI†). The formation of metallic tellurium indicates reduction of the Te^{VI} in **1** to Te⁰ as the cluster decomposed. The apparent chemical conversion of the niobate cluster is also reflected in the non-linear H₂ evolution plot, which shows an abrupt increase of activity after 2 h. The main product of the photo-assisted

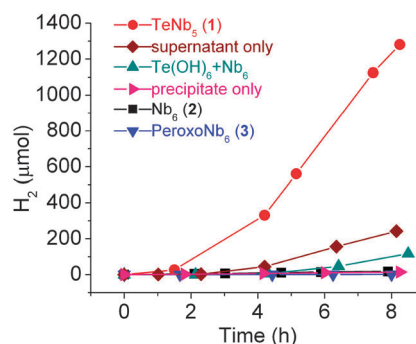
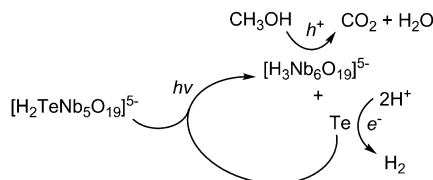


Fig. 3 Hydrogen evolution data in 20% (v/v) methanol–water solution (25 mL) during the irradiation from full spectrum of Xe lamp.



Scheme 1 Proposed photocatalytic reaction mechanism.

conversion of 1–3 in the solution phase after irradiation was the Nb₆ ion, as detected by ESI-MS. The peroxohexaniobate ion 3 showed lowest H₂ evolution activity (1 μmol h⁻¹ g⁻¹) when compared to 1 and 2, but evolved small amounts of O₂ during irradiation, likely due to the photo-induced removal of the peroxo ligand.

The supernatant and precipitate were separated after irradiation of solution of 1 for 8 h to evaluate the H₂-evolution activity of each photo-decomposition product separately. Te⁰ wires alone showed very low H₂ evolution activity when mixed with water-methanol [Fig. 3]. The separated supernatant continued to form more Te⁰ upon irradiation due to the small amount of tellurate present in the supernatant. This supernatant showed a similar H₂ evolution curve but lower H₂ evolution activity than the original solution [Fig. 3] probably due to the smaller amount of precipitate, suggesting that coexistence of the niobate cluster and metallic Te⁰ is necessary to maintain the high H₂ evolution activity.

These results suggest a mechanism for photocatalytic H₂ evolution shown in Scheme 1. Photoexcitation of TeNb₅ forms an electron-hole pair and the electron reduces Te^{VI} in the cluster. As a result, TeNb₅ is decomposed to Te⁰ and Nb₆ with the hole oxidizing methanol as a sacrificial electron donor, ultimately forming CO₂ and H₂O. Once Te^{VI} is fully reduced to Te⁰, it may further accept electrons to become telluride (Te²⁻). We speculate that this aqueous telluride will reduce protons to evolve H₂, as H₂Te has been shown to decompose to metallic tellurium in aqueous solution.¹⁰ Thus we believe that the high H₂ evolution activity in this system is due to coexistence of Nb₆ and Te⁰ nanowires or colloids and that the native tellurium metal acts as a H₂-evolution cocatalyst. Cobaloxime or H₂PtCl₆ has been commonly used as a cocatalyst in the study of H₂ evolution from polyoxoniobate and many other systems.^{6c,8} To our knowledge, this is the first demonstration of Te⁰ as a H₂ evolution cocatalyst.

For control experiments, stoichiometric mixtures of telluric acid and 2 (Te:Nb = 1:5) were tested for H₂ evolution. Nearly the same amount (~10 mg) of Te⁰ formed in this solution after irradiation, but the amount of H₂ evolved (71 μmol h⁻¹ g⁻¹) was about an order of magnitude smaller than that produced from the solution of 1, but higher than that produced from the solution of 2 alone [Fig. 3]. This result implies that the reduction of Te^{VI} in TeNb₅ can occur directly within the cluster from the photogenerated electron-hole pairs, in such a way that formation of metallic tellurium in the solution of 1 is faster than in the simple solution mixture of telluric acid and 2. This explains the high H₂ evolution rate in the early stage of

irradiation of 1 compared to the control experiment. The total surface area of the particles in the solution of 1 might also be higher than that in the mixture of telluric acid and 2 because of the faster formation of particles, which might have resulted in the high H₂-evolution activity.

In conclusion, the TMA salt of the TeNb₅ molecule reported herein exhibits a similar pH stability window and solid-state structure compared to Nb₆, but demonstrates much higher H₂-evolution activity *via* a photo-decomposition route to Nb₆ and Te⁰ nanowires. Future studies shall focus on the hydrolysis and isotope-exchange kinetics of the TeNb₅ molecule, by using ¹⁷O and ¹²⁵Te NMR together, and compare hydrolysis chemistry with that of the unsubstituted Nb₆.

This work was supported by an NSF CCI grant through the Center for Sustainable Materials Chemistry, number CHE-1102637.

Notes and references

‡ Crystal data. (1) CCDC 959006. C₂₀H₉₄N₅O_{39.25}TeNb₅, *M* = 1625.15, monoclinic, *a* = 33.8700(15) Å, *b* = 8.4954(4) Å, *c* = 21.9238(10) Å, β = 110.475(1)°, *U* = 5909.8(5) Å³, *T* = 93 K, space group *C2/c* (no. 15), *Z* = 4, 31 567 reflections measured, 6782 unique (*R*_{int} = 0.0218) which were used in all calculations. The final *wR*(*F*²) was 0.0407 (all data).

- (a) I. Lindqvist, *Ark. Kemi*, 1953, **5**, 247–250; (b) E. J. Graeber and B. Morosin, *Acta Crystallogr., Sect. B*, 1977, **33**, 2137–2143; (c) S. Si Larbi, D. Bodiot and B. Spinner, *Rev. Chim. Miner.*, 1976, **13**, 497–507; (d) A. Goiffon and B. Spinner, *Talanta*, 1977, **24**, 130–132; (e) M. Nyman, *Dalton Trans.*, 2011, **40**, 8049–8058.
- V. W. Day, W. C. Klemperer and C. Schwartz, *J. Am. Chem. Soc.*, 1987, **109**, 6030–6044.
- (a) T. M. Alam, M. Nyman, B. R. Cherry, J. M. Segall and L. E. Lybarger, *J. Am. Chem. Soc.*, 2004, **126**, 5610–5620; (b) J. R. Black, M. Nyman and W. H. Casey, *J. Am. Chem. Soc.*, 2006, **128**, 14712–14720.
- (a) I. L. Botto, C. I. Cabello and H. J. Thomas, *Mater. Chem. Phys.*, 1997, **47**, 37–45; (b) P. A. Lorenzo Luis, P. Martin-Zarza, A. Sanchez, C. Ruiz-Pérez, M. Hernández-Molina, X. Solans and P. Gili, *Inorg. Chim. Acta*, 1998, **277**, 139–150; (c) D. Drewes, E. M. Limanski and B. Krebs, *Eur. J. Inorg. Chem.*, 2004, 4849–4853; (d) D. Drewes and B. Krebs, *Z. Anorg. Allg. Chem.*, 2005, **631**, 2591–2594; (e) J. Wang, G. Zhang, P. Ma and J. Niu, *Inorg. Chem. Commun.*, 2008, **11**, 825–828.
- (a) R. I. Maksimovskaya, V. M. Bondareva and G. I. Aleshina, *Eur. J. Inorg. Chem.*, 2008, 4906–4914; (b) S. Konaka, Y. Ozawa and A. Yagasaki, *Inorg. Chem. Commun.*, 2008, **11**, 1267–1269; (c) S. Konaka, Y. Ozawa, T. Shonaka, S. Watanabe and A. Yagasaki, *Inorg. Chem.*, 2011, **50**, 6183–6188.
- (a) Y. Ebina, A. Tanaka, J. N. Kondo and K. Domen, *Chem. Mater.*, 1996, **8**, 2534–2538; (b) A. Kudo, H. Kato and S. Nakagawa, *J. Phys. Chem. B*, 2000, **104**, 571–575; (c) F. Osterloh, *Chem. Mater.*, 2008, **20**, 35–54; K. Akatsuka, G. Takanashi, Y. Ebina, M. Haga and T. Sasaki, *J. Phys. Chem. C*, 2012, **116**, 12426–12433.
- A. G. S. Prado, L. B. Bolzon, C. P. Pedroso, A. O. Moura and L. L. Costa, *Appl. Catal., B*, 2008, **82**, 219–224.
- (a) Z. Zhang, Q. Lin, D. Kurunthu, T. Wu, F. Zuo, S.-T. Zheng, C. J. Bardeen, X. Bu and P. Feng, *J. Am. Chem. Soc.*, 2011, **133**, 6934–6937; (b) P. Huang, C. Qin, Z.-M. Su, Y. Xing, X.-L. Wang, K.-Z. Shao, Y.-Q. Lan and E.-B. Wang, *J. Am. Chem. Soc.*, 2012, **134**, 14004–14010; (c) Z.-L. Wang, H.-Q. Tan, W.-L. Chen, Y.-G. Li and E.-B. Wang, *Dalton Trans.*, 2012, **41**, 9882–9884.
- C. A. Ohlin, E. M. Villa, J. C. Fettingier and W. H. Casey, *Angew. Chem., Int. Ed.*, 2008, **47**, 8251–8254.
- L. M. Dennis and R. P. Anderson, *J. Am. Chem. Soc.*, 1914, **36**, 882–909.

